Quantum billiards and constrained random wave correlations

W E Bies[1]**, N Lepore**[1] **and E J Heller**[2]

[1] Department of Physics, Harvard University, Cambridge, MA 02138, USA
[2] Department of Physics and Department of Chemistry, Harvard University, Cambridge,
MA 02138, USA

Abstract
We study chaotic eigenfunctions in wedge-shaped and rectangular regions
using a generalization of Berry's conjecture. An expression for the two-point
correlation function is derived and verified numerically.

PACS numbers: 03.65.−w, 05.45.Mt

1. Introduction

According to Berry's conjecture [1], chaotic eigenfunctions behave locally like random
superpositions of plane waves with wave vector k, where $k = (1/\hbar)\sqrt{E - V}$. This description
is consistent with random matrix theory. The Gaussian random wave model does not account
for the localization properties of eigenfunctions, such as scarring [2] and weak quantum
ergodicity [3]. In particular, for quantum billiards with Dirichlet boundary conditions, the
wavefunction must vanish at the boundary, and thus no longer looks random in its vicinity. For
straight boundaries, the problem can be solved by reducing the set of available plane waves
to those which are antisymmetric with respect to reflection across the wall, thereby ensuring
a zero value along that boundary; see Berry [4]. If, for instance, the boundary is given by the
line $y = 0$, the chaotic wavefunction will be composed of a seemingly random combination
of plane waves of the form $\sin(k_y y) \cos(k_x x + \phi)$ where $k_x^2 + k_y^2 = k^2$ and ϕ is a random phase
shift. Bies and Heller [5] discuss similar boundary effects in soft potentials.

Some criteria for unconfined random waves appear to be well satisfied by eigenfunctions
of chaotic billiards. McDonald and Kaufman [6] and McDonald [7] checked for random
nodal patterns, Gaussian statistics and Bessel function correlations. In their original work
on the stadium, these authors emphasized the qualitative appearance of nodal lines in the
eigenfunctions. The nodal lines appear to wander randomly throughout the billiard, which
is indicative of an isotropic distribution of local wave vectors. Furthermore, they found the
wavefunction statistics to be Gaussian. However, the correlation function is not a Bessel
function for a general billiard.

We first generalize Berry's boundary-adapted form of the Gaussian random wave model to wedge-shaped regions. The case of a $90°$ angle is immediately solved: one just antisymmetrizes with respect to reflections in both x and y. The simplest non-trivial case consists of a wedge with an opening angle of $60°$. We focus on this example in what follows, although our method extends to all opening angles of π/n radians, where n is a positive integer. We first determine the right boundary-adapted plane wave basis. The two-point correlation function can be used to compare our model to numerically generated chaotic eigenstates. For Gaussian random waves in free space, the latter is known to give

$$\langle \psi(\mathbf{x}) \bar{\psi}(\mathbf{x}') \rangle = J_0(|\mathbf{x} - \mathbf{x}'|) \tag{1}$$

where the average is taken over a set of eigenstates. As we shall see, the two-point correlation function for $60°$ wedge again reduces to a sum of Bessel functions. Our numerically generated ensemble of wavefunctions is compared to this form of the correlation function, including the interference effects of two or more Bessel functions.

Our second type of billiard consists of two semi-infinite parallel lines at $x > 0$, $y = \pm a/2$, which are connected by a perpendicular wall at $x = 0$. The wavefunction can be made to vanish on the back wall by antisymmetrizing it with respect to the y-axis. The parallel walls are not so readily handled. The antisymmetrization procedure extends over an infinite periodic array of such lines a distance a apart. The two-point correlation function will be composed of an infinite sum of Bessel functions. Since the latter diminish rapidly with distance, only the nearest neighbours contribute, allowing us to compare our formula with its numerically determined value.

2. The two-point correlation function

2.1. The wedge

We first look for the properly antisymmetrized wavefunctions. Let

$$\psi(\mathbf{x}) = \int \mathrm{d}\theta\, a_\theta\, \mathrm{e}^{-\mathrm{i}\mathbf{k}_\theta \cdot \mathbf{x} + \mathrm{i}\delta_\theta} \tag{2}$$

denote a random sum of plane waves. Here $\mathbf{k}_\theta = k\cos\theta\,\hat{\mathbf{x}} + k\sin\theta\,\hat{\mathbf{y}}$, the a_θ are independent Gaussian distributed random variables and the δ_θ are independent uniformly distributed random phase shifts. Let $\tilde{\psi}(\mathbf{x})$ denote the desired boundary-adapted version of $\psi(\mathbf{x})$. Since $\tilde{\psi}(\mathbf{x})$ vanishes on the boundary of the wedge, it can be extended to a fictitious wavefunction living in the whole plane by reflecting antisymmetrically across either boundary. To obtain $\tilde{\psi}(\mathbf{x})$, we let R_1 denote reflection with respect to one of the lines bounding the wedge and R_2 reflection with respect to the other line. We would like to antisymmetrize $\psi(\mathbf{x})$ with respect to both of these reflections. The projection operator $(1/4)(1 - R_1)(1 - R_2)$ does not work, however, because R_1 and R_2 do not commute. Instead, we must resort to the following group-theoretical construction. Let R_3 denote the reflection with respect to the line that passes through the vertex of the wedge and meets the two edges of the wedge at a $60°$ angle. The product $R_1 R_2$ of the two reflections R_1 and R_2 is a rotation through $120°$ centred on the vertex, and $R_2 R_1$ is the opposite rotation. Thus, the set $1, R_1, R_2, R_3, R_1 R_2, R_2 R_1$ forms a representation of the dihedral group C_3. It is now easy to see that $\tilde{\psi}(\mathbf{x})$ transforms under the one-dimensional representation of C_3 that assigns a character of -1 to the reflections and 1 to the rotations. Put another way, the problem of going from $\psi(\mathbf{x})$ to $\tilde{\psi}(\mathbf{x})$ is that of projecting onto this irreducible representation of C_3. Formally, this transformation is expressed as [8]

$$\tilde{\psi}(\mathbf{x}) = \frac{1}{\sqrt{6}} \sum_{A \in C_3} \chi(A) A \psi(\mathbf{x}). \tag{3}$$

Here, A denotes the group elements $1, R_1, R_2, R_3, R_1 R_2$ and $R_2 R_1$, and the character is given by $\chi(R_1) = \chi(R_2) = \chi(R_3) = -1$ and $\chi(1) = \chi(R_1 R_2) = \chi(R_2 R_1) = 1$. The normalization factor of $1/\sqrt{6}$ is chosen to ensure that the two-point correlation function gives the free-space result far away from the wall. If we then restrict $\tilde{\psi}(\mathbf{x})$ to the wedge-shaped region, we obtain the required boundary-adapted sum of plane waves.

Now that we have an explicit expression for $\tilde{\psi}(\mathbf{x})$, we can use it to calculate the two-point correlation function $C(\mathbf{x}, \mathbf{x} + \mathbf{r}) = \langle \tilde{\psi}(\mathbf{x}) \bar{\tilde{\psi}}(\mathbf{x} + \mathbf{r}) \rangle$. The correlation function is a sum of 36 terms of the form

$$\langle \chi(A) A \psi(\mathbf{x}) \chi(B) B \bar{\psi}(\mathbf{x} + \mathbf{r}) \rangle = \chi(A) \chi(B) \int d\theta \, e^{-i\mathbf{k}_\theta \cdot (A\mathbf{x} - B\mathbf{x}) + i\mathbf{k}_\theta \cdot B\mathbf{r}} \tag{4}$$

$$= \chi(A) \chi(B) \int d\theta \, e^{ik\rho \cos(\theta - \theta_0)} \tag{5}$$

$$= \chi(A) \chi(B) J_0(k\rho). \tag{6}$$

Here $\rho = |A\mathbf{x} - B(\mathbf{x} + \mathbf{r})|$, that is, the distance from $\mathbf{x} + \mathbf{r}$ to $B^{-1}A\mathbf{x}$. The correlation function becomes

$$C(\mathbf{x}, \mathbf{x} + \mathbf{r}) = \frac{1}{6} \sum_{A,B \in C_3} \chi(A) \chi(B) J_0(k\rho_{B^{-1}A}) \tag{7}$$

$$= \sum_{C \in C_3} \chi(C) J_0(k\rho_{C^{-1}}) \tag{8}$$

$$= J_0(kr) - J_0(k\rho_{R_1}) - J_0(k\rho_{R_2}) - J_0(k\rho_{R_3}) + J_0(k\rho_{R_1 R_2}) + J_0(k\rho_{R_2 R_1}). \tag{9}$$

In the second line, we replaced B by AC. The sum over A then becomes trivial, since $\chi(A) \chi(B) = \chi(A) \chi(A) \chi(C) = \chi(C)$. In the last line, ρ_A denotes the distance from $\mathbf{x} + \mathbf{r}$ to $A\mathbf{x}$.

This formula predicts that the two-point correlation function should display the interference of Bessel functions centred at all the points given by applying the group transformations on $\mathbf{x}$. Far from the boundary, equation (7) reduces to the single Bessel function $J_0(kr)$, the value that it would have if no boundary were present. However, the interference is pronounced near the boundary, and more especially near the vertex of the wedge.

2.2. The rectangular corridor

In the case of the rectangular corridor, the back wall and the semi-infinite walls need to be handled separately. The wavefunction at $\mathbf{x}$ in the $x < 0$ half-plane is obtained by reflecting about the y-axis. To extend the wavefunction in the y direction, we reflect it with respect to the wall at $y = a/2$. By repeating this process for all $y = (1 + 2m)a/2$ where $m = \{\ldots, -1, 0, 1, \ldots\}$, the whole plane is tiled with positive or negative copies of $\psi(\mathbf{x})$.

Mathematically, the process by which $\tilde{\psi}(\mathbf{x})$ is obtained is as follows. The initial billiard is placed on an infinitely long cylinder of circumference $2an$. Our initial x-axis is now parallel to the axis of the cylinder, whereas the y-axis is wrapped around the cylinder and truncated at $y = (1 \pm 2n)a/2$. The wavefunction is first reflected across the y-axis. Therefore, the antisymmetrization in the x direction transforms as a one-dimensional representation of the reflection group $\mathbf{Z_2}$. Rotations by multiples of $2a$ should give back the wavefunction, while reflections about any of the lines parallel to the x-axis give its negative version. We thus obtain a representation of the dihedral group C_n. It is now clear that on the cylinder, $\tilde{\psi}(\mathbf{x})$
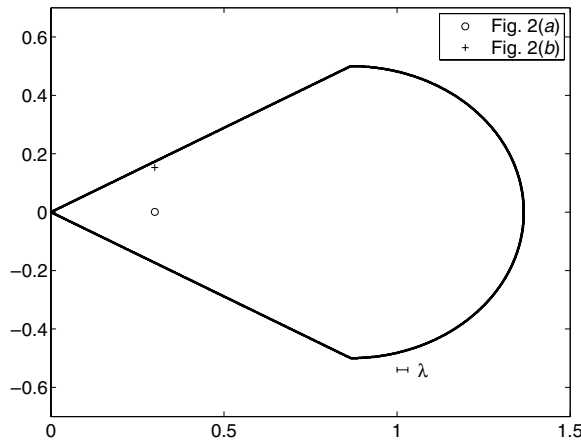
Figure 1. The cone billiard.

transforms under the one-dimensional representation of $C_n \otimes \mathbf{Z_2}$ that assigns a character of -1 for reflections and 1 for rotations. This time the transformation is given by

$$\tilde{\psi}_n(\mathbf{x}) = \frac{1}{\sqrt{4n}} \sum_{A \in C_n \otimes \mathbf{Z_2}} \chi(A) A \psi(\mathbf{x}). \tag{10}$$

As in the case of the wedge, the normalization factor is found by requiring that the correlation function give $J_0(k\rho)$ far away from the wall.
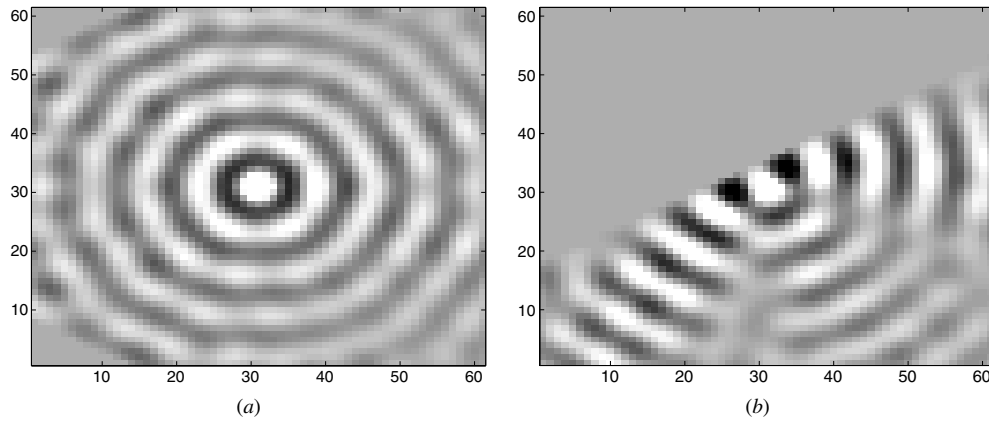
The correlation function is given by

$$C(\mathbf{x}, \mathbf{x} + \mathbf{r}) = \lim_{n \to \infty} \frac{1}{4n} \sum_{A, B \in C_n \otimes \mathbf{Z_2}} \chi(A) \chi(B) J_0(k\rho_{B^{-1}A}) \tag{11}$$

$$= \lim_{n \to \infty} \sum_{C \in C_n \otimes \mathbf{Z_2}} \chi(C) J_0(k\rho_{C^{-1}}). \tag{12}$$

However, $J_0(k\rho_{C^{-1}}) \to 1/\sqrt{k\rho_{C^{-1}}}$ for large $\rho_{C^{-1}}$. Hence, only the Bessel functions centred at nearby points contribute, and the correlation function remains finite as we take the $n \to \infty$ limit.

3. Numerical results

Here we apply the theory to check further the properties of random waves in billiard systems. There are some obvious and some more subtle modifications of random wave behaviour known in closed chaotic billiards. The wavefunction must vanish on the boundary, and scarring affects some states in a non-random way [9]. The theory given here suggests new correlations which ought to be checked in chaotic systems. As we incorporate more about a specific billiard geometry into our correlation functions, we are probing the properties of waves which are 'as random as possible' within the constraints, such as a wedge boundary being present. In checking the numerics of a billiard such as the cone or stadium, we are really asking whether the eigenstates are truly random but for the constraint of interest, say a wedge boundary. Naturally this cannot be strictly true, since there are more constraints that we have not included. At the end of this strategy comes a tautology: if, in a closed billiard we incorporate *all* the constraints, we have only the eigenstates left, as the *only* waves which are consistent with all the constraints!

Figure 2. (*a*) Experimental correlation function for $\mathbf{x} = (0.3, 0)$, on the symmetry axis through the centre of the cone. The grid is a square of side 0.129, or about eight wavelengths, centred on $\mathbf{x}$. (*b*) Same as (*a*) for $\mathbf{x} = (0.3, 0.153)$, near the upper straight edge of the cone.
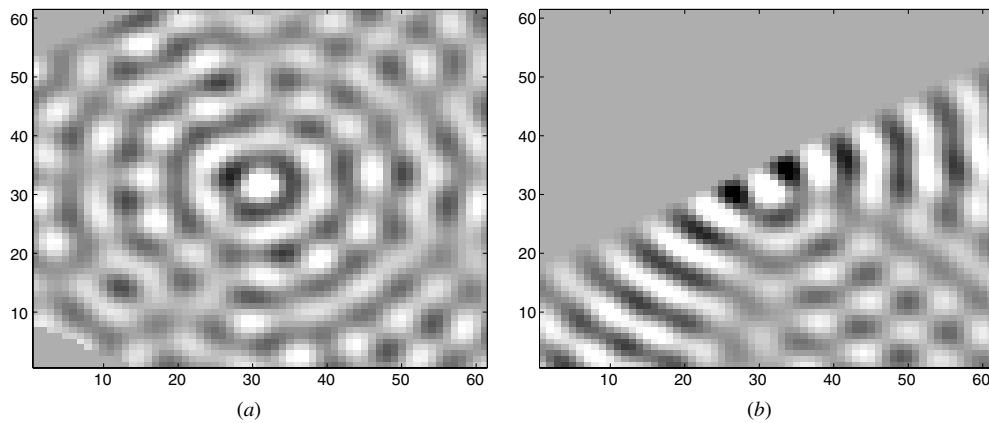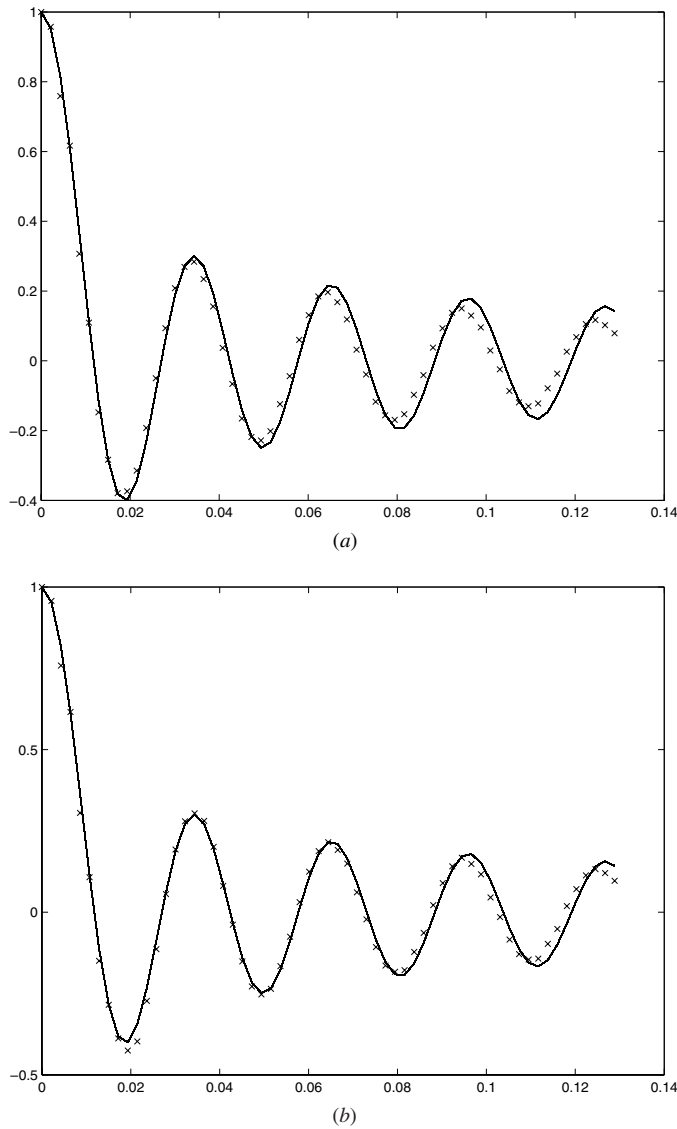

Figure 3. (*a*) Theoretical correlation function for $\mathbf{x} = (0.3, 0)$ (same grid as in figure 2(*a*)). (*b*) Same as (*a*) for $\mathbf{x} = (0.3, 0.153)$ (same grid as in figure 2(*b*)).

3.1. The wedge

To validate our expressions for $\tilde{\psi}(\mathbf{x})$ and $C(\mathbf{x}, \mathbf{x} + \mathbf{r})$, we generated an ensemble of 500 eigenstates near $k = 200$ for a $60°$ wedge which has been closed off by a semicircle; see figure 1. The eigenstates were found using the Boundary Integral Method. Our cone-shaped billiard has a circle diameter equal to 1, which is about 32 wavelengths across. The Poincaré section indicates that this billiard is chaotic. In figure 2, we show $C(\mathbf{x}, \mathbf{x} + \mathbf{r})$ for (*a*) $\mathbf{x}$ on the symmetry line through the centre of the billiard and (*b*) for $\mathbf{x}$ placed within a wavelength of one of the edges. Both figures 2(*a*) and (*b*) display the expected interference, but the latter is especially pronounced in figure 2(*b*). Note that since $\mathbf{x}$ is on the symmetry line, only even states contribute to figure 2(*a*).

For comparison, figure 3 displays the theoretical predictions for the two-point correlation functions of figure 2. Both plots are in good agreement with their numerical equivalent. In particular, the interference pattern of figure 2(*b*) is reproduced in figure 3(*b*). However, the angular oscillations are much more pronounced in the theoretical plots, suggesting that an

Figure 4. (*a*) Angular average of $C(\mathbf{x} + \mathbf{r}, \mathbf{x})$ versus r for $\mathbf{x} = (0.3, 0)$ (same grid as in figure 2(*a*)). Solid line, Bessel function $J_0(kr)$; $\times$, numerical data. (*b*) Same as (*a*) for $\mathbf{x} = (0.3, 0.153)$ (same grid as in figure 2(*b*)).

unaccounted-for smoothing process is at work in the numerical experiment. We compared the error quantitatively using

$$\frac{\int \mathrm{d}^2 r |C_{\mathrm{num}}(\mathbf{x}, \mathbf{x} + \mathbf{r}) - C_{\mathrm{th}}(\mathbf{x}, \mathbf{x} + \mathbf{r})|^2}{\int \mathrm{d}^2 r C_{\mathrm{th}}(\mathbf{x}, \mathbf{x} + \mathbf{r})^2}. \tag{13}$$

We obtained 0.52 for figure 2(*a*) and 0.15 for figure 2(*b*). The discrepancy in the predicted and experimental values is expected due to the difference in the angular nodes, and appears to be more pronounced far away from the billiard walls.

In figure 4, we take the angular average of the correlation functions of figure 2. As was found by Li and Robnik [10], figure 4(*a*) resembles the Bessel function $J_0(kr)$. This should
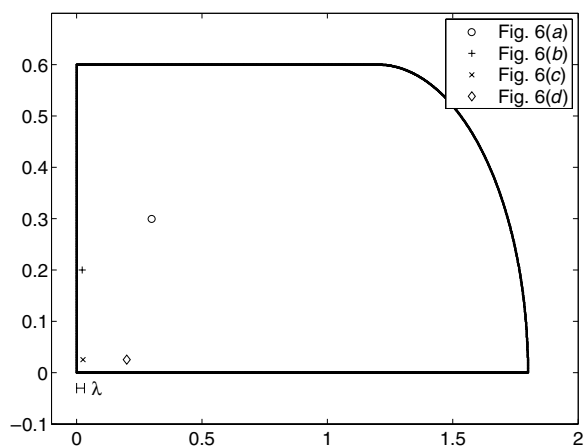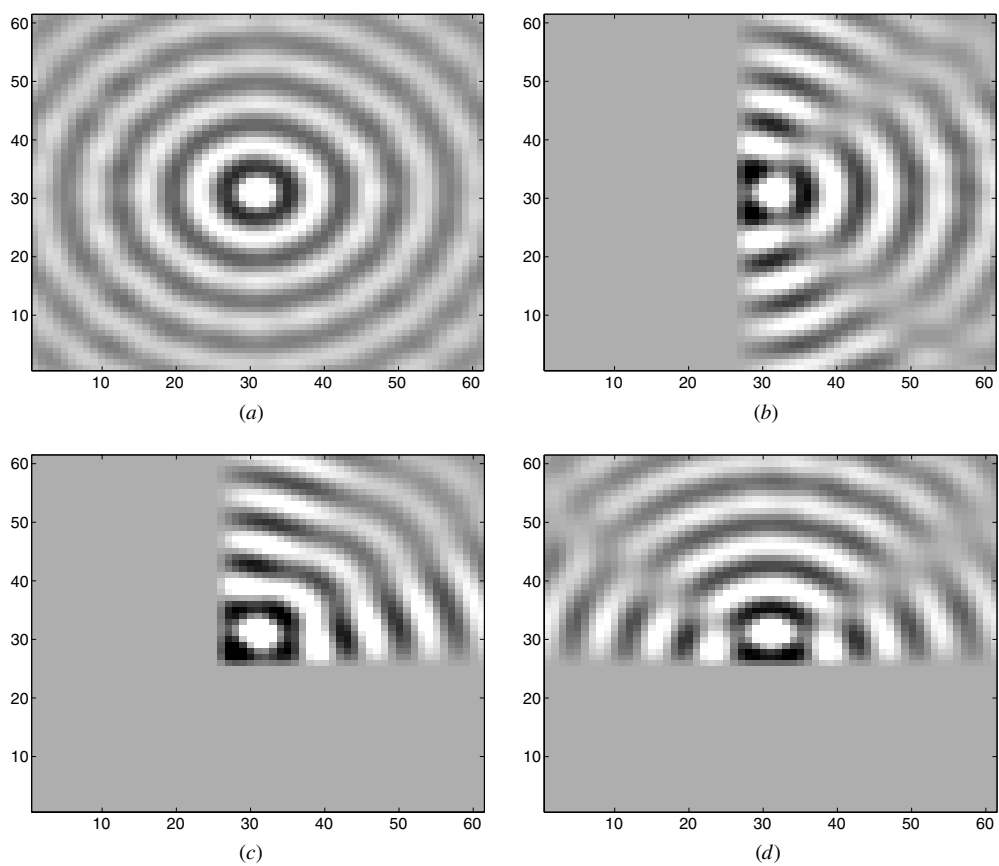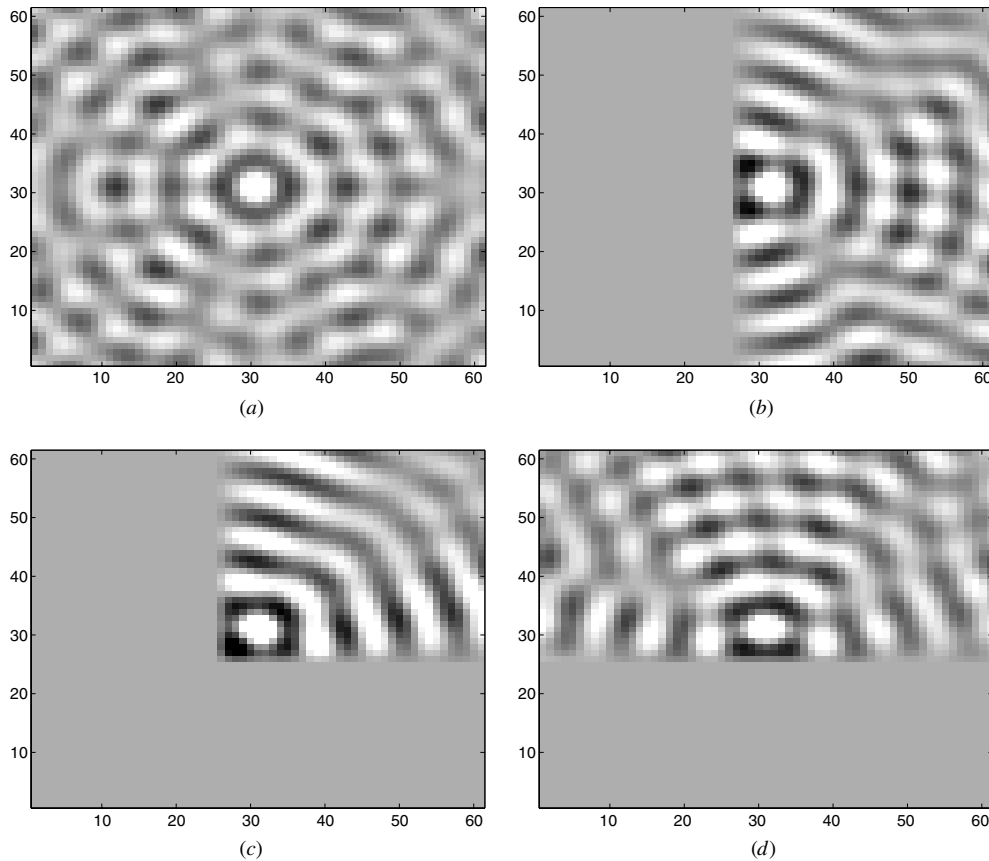
Figure 5. The stadium billiard.

Figure 6. (a) Experimental correlation function for **x** = (0.3, 0.3), the midpoint of the square part of the stadium. The grid is a square of side 0.140, or about eight wavelengths, centred on **x**. (b) Same as (a) for **x** = (0.0223, 0.2), near the back wall. (c) Same as (a) for **x** = (0.0255, 0.0255), near the lower-left corner. (d) Same as (a) for **x** = (0.2, 0.0255), near the bottom side of the stadium.

Figure 7. (*a*) Theoretical correlation function for $\mathbf{x} = (0.3, 0.3)$ (same grid as in figure 6(*a*)). (*b*) Same as (*a*) for $\mathbf{x} = (0.0223, 0.2)$ (same grid as figure 6(*b*)). (*c*) Same as (*a*) for $\mathbf{x} = (0.0255, 0.0255)$ (same grid as figure 6(*c*)). (*d*) Same as (*a*) for $\mathbf{x} = (0.2, 0.0255)$ (same grid as figure 6(*d*)).

be the case whenever boundary effects contribute equally from all sides. Figure 4(*b*) also approximates a Bessel function because, as can be seen from figure 2(*b*), the boundary effects affect only a small range of angles and, furthermore, are independent of radius.

3.2. The rectangular corridor

Once again, we took an ensemble of 500 eigenstates near $k = 200$, this time for a quarter stadium with an end cap radius of $R = 0.6$ and straight length $l = 1.2$ (about 20 wavelengths wide), see figure 5. The numerical correlation function is shown in figure 6 for $\mathbf{x}$ (*a*) on the symmetry line through the centre of the billiard, (*b*) within one wavelength of the top wall, (*c*) within one wavelength of a corner and (*d*) within one wavelength of the back wall. As expected, only the Bessel functions which are less than a few wavelengths away contribute to $C(\mathbf{x}, \mathbf{x} + \mathbf{r})$.

The numerical correlation function of figure 6 was compared to the theoretical prediction of figure 7 using equation (13). Here, only the first few terms were kept in $C_{\text{th}}(\mathbf{x}, \mathbf{x} + \mathbf{r})$. We obtain 0.55 for figure 6(*a*), 0.23 for figure 6(*b*), 0.03 for figure 6(*c*) and 0.24 for figure 6(*d*), in agreement with our results for the cone billiard.

4. Conclusion

We have successfully extended the boundary-adapted Gaussian wave model to a wedge-shaped region with opening angle $60°$. Our technique is readily generalized to any opening angle of the form π/n for n integer; one merely replaces the group elements of C_3 with those of the dihedral group C_n. We also solved the case of the semi-infinite rectangular corridor. It is our hope that these results will stimulate more work on boundary effects in arbitrarily shaped billiards; in particular, it would be desirable to compare our semiclassical expression of Hortikar and Srednicki [11].

Acknowledgments

References

[1] Berry M V 1983 *Chaotic Behaviour of Deterministic Systems* ed G Iooss, R Helleman and R Stora (Amsterdam: North-Holland) p 171
[2] Heller E J 1984 *Phys. Rev. Lett.* **53** 1515
[3] Kaplan L and Heller E J 1998 *Physica* D **121** 1
[4] Berry M V 2002 *J. Phys. A: Math. Gen.* **35** 3025
[5] Bies W E and Heller E J 2002 *J. Phys. A: Math. Gen.* **35** 5673
[6] McDonald S W and Kaufman A N 1988 *Phys. Rev.* A **37** 3067
[7] McDonald S W *PhD Thesis* University of California, Lawrence Berkeley Laboratory, 1983 (Report no 14837, unpublished)
[8] Tinkham M 1964 *Group Theory and Quantum Mechanics* (New York: McGraw-Hill)
[9] Kaplan L and Heller E J 1998 *Ann. Phys., NY* **264** 171
Kaplan L 1998 *Phys. Rev. Lett.* **80** 2582
[10] Li B and Robnik M 1994 *J. Phys. A: Math. Gen.* **27** 5509
[11] Hortikar S and Srednicki M 1998 *Phys. Rev. Lett.* **80** 1646